Supporting information

Parahydrogen hyperpolarization of minimally altered urine samples for sensitivity enhanced NMR metabolomics

Kerti Ausmees, Nele Reimets and Indrek Reile

National Institute of Chemical Physics and Biophysics
Akadeemia tee 23
Tallinn 12618
Estonia

Table of Contents

1.   Sample collection and handling

Urine sample handling was approved by the Estonian Research Ethics Committee of the National Institute for Health Development of Estonia (Decision No 686). Urine samples used in this research were donated by healthy adults (30-40 years of age). One adult was a smoker. Informed consent was obtained from all participating persons. Donated urine samples were collected as morning first midstream urine and used for sample preparation or frozen within 2 h. Stored samples were kept at -80 °C. Frozen samples were allowed to thaw over a room temperature water bath prior to sample preparation. Excess urine sample material was discarded in accordance with local regulations on handling human derived samples.

2.   Chemicals and materials

The active catalyst precursor [Ir(Cl)(COD)(IMes)] was synthesized in house according to a published procedure.[1,2] The catalyst system co-substrate 1-methyl-1,2,3-triazol (mtz) was synthesized according to a published procedure.[3] All other chemicals were purchased from common chemical suppliers: nicotine (99+%, nic, Acros Organics), cotinine (≥98%, cot, Alfa Aesar), N1-methyladenosine (≥98%, m1a, Cayman Chemicals), adenine hemisulfate (≥98%, ade, Cayman Chemicals), *trans*-3'-hydroxycotinine (≥98%, 3hc, Cayman Chemicals), nicotinamide (99+%, nam, TCI Chemicals), guanosine (≥98%, gua, TCI Chemicals), adenosine (≥99%, a, TCI Chemicals), N6-methyladenosine (m6a, Carbosynth), 2,2-dimethyl-2-silapentane-5-sulfonate (DSS, Eurisotop).

NMR experiments were carried out on an 800 MHz Bruker Avance III spectrometer equipped with a He-cooled 5 mm cryoprobe. The spectrometer was operating under Topspin 3.5pl6 acquisition software. Soft pulses for hyperpolarization experiments were generated with the Bruker Wavemaker plugin. Parahydrogen was produced in flow in a previously described setup.[4] The experimental setup for parahydrogen hyperpolarization consisted of a "bubbling control box" spectrometer accessory that allows parahydrogen bubbling through the NMR sample under pulse program control. The setup and its operation principles have been published earlier.[4]

Processing of 1D and 2D NMR data was done in MestReNova 14.2.1. Due to the limited configurability of convolution filtering in MestReNova, convolution filtering was applied to raw data in Bruker Topspin, with the rest of processing carried out as usual in MestReNova.

3. Urine sample preparation

Fresh or thawed urine was centrifuged at 1825 g for 12 min, pH adjusted to appropriate level with 1 M NaOH aq, and centrifuged again. Resulting clear yellow supernatant was used for further sample preparation prior to analysis:

a) *For pH optimization in ammonia stripping (Fig. 2 in main text):* 600 μL of pH adjusted urine was added to Eppendorf tubes, frozen in liquid nitrogen and dried in a MiVac Speedvac rotary vacuum concentrator for 48 h. NMR samples were prepared by adding 600 μL of methanol-d_4 to the concentrate, sonicating the mixture for 10 minutes and centrifuging again at 1825 g for 3 min. Resulting clear yellow supernatant was used for hyperpolarization experiments (see section 4a below).

b) *For concentrated urine sample preparation (Fig. 1b and 3 in main text):* urine was pH adjusted to 11 with 1 M NaOH aq, centrifuged and 2.4 mL of the supernatant was loaded to a centrifuge tube, frozen in liquid nitrogen and lyophilized for 48 h. Dry urine residues were stored at -80 °C until analysis. NMR samples were prepared by adding 150 μL of D_2O to the residue and allowed to dissolve, yielding a dark yellow liquid. Salts and residual proteins were precipitated by adding 450 μL of methanol-d_4. After 10 minutes of sonication, the mixture was centrifuged at 1825 g for 3 min and the methanol-d_4 layer was used in hyperpolarization experiments (see section 4b below).

c) *Enzymatic urease treatment* of urine was carried out in accordance to a literature procedure.[5]

d) *Preparing stock solutions of internal standards:* All solutions were prepared gravimetrically. Appropriate amounts of standard chemicals (see section 2 above) were separately dissolved in methanol-d_4 to obtain 10 mM stock solutions of each. Solutions were further diluted in methanol-d_4 to obtain 1 mM, and 0.1 mM stock solutions, which were spiked into hyperpolarization samples.

e) A gravimetrically prepared 100 mM solution of DSS sodium salt in D_2O was used as internal standard for determining NH_4^+ concentration in urine samples (section 5 below).

4. NMR sample preparation and NMR experiments

a) *Preparing 1.2 mM catalyst system solutions (for Fig. 2 in main text):*

The active pH_2-HP catalyst [Ir(H_2)(IMes)(mtz)$_3$]Cl, was prepared *in situ* in an NMR tube. 150 μL of a stock solution of [Ir(Cl)(COD)(IMes)] (4.8 mM in methanol-d_4) and 12 μL of a stock solution of 1-methyl-1,2,3-triazole (mtz, 1 M in methanol-d_4) co-substrate were loaded into a 5 mm Norell IPV NMR tube, pressurized under 5 bar of H_2, shaken, and allowed to react at room temperature for 2 h, before adding appropriate amounts of methanolic urine sample (e.g., 60 μL; see section

3a above) and neat methanol-d_4 to reach 600 µL of liquid in the NMR tube. The final concentrations were 1.2 mM for [Ir(H$_2$)(IMes)(mtz)$_3$]Cl and 20.4 mM for mtz.

b) Preparing 6 mM catalyst system solutions (for Fig. 1b, 3 and 4 in main text):
The active pH$_2$-HP catalyst [Ir(H$_2$)(IMes)(mtz)$_3$]Cl, was prepared *in situ* in an NMR tube. 300 µL of a stock solution of [Ir(Cl)(COD)(IMes)] (12 mM in methanol-d_4) and 65 µL of a stock solution of 1-methyl-1,2,3-triazole (mtz, 1 M in methanol-d_4) co-substrate were measured into a 5 mm Norell IPV NMR tube, pressurized under 5 bar of H$_2$, shaken, and allowed to react for 2 h before adding appropriate amounts (e.g., 30 µL, see section 3b above) of methanolic urine sample and neat methanol-d_4 to reach 600 µL of liquid in NMR tube. The final concentrations were 6 mM for [Ir(H$_2$)(IMes)(mtz)$_3$]Cl and 102.3 mM for mtz.

The IPV tubes were connected to the HP setup[4] (see section 2 above) after adding the sample, re-pressurized under 5 bar of H$_2$ and inserted into the NMR spectrometer. Hyperpolarization was facilitated by bubbling parahydrogen through the sample under pulse program control. 1D and 2D pH$_2$-HP spectra were recorded at 15 or 25 °C sample temperature.

Hyperpolarized 1D hydride spectra (Figures 1b and 2 in main text) were acquired in 128 transients, each involving refreshment of dissolved parahydrogen during 2 s of gas bubbling through the sample. The in-phase 1D spectra of the hyperpolarized parahydrogen derived hydrides were acquired with a previously published adaption[6] of the SEPP[7,8] pulse sequence.

Hyperpolarized 2D spectra were acquired with the previously publish<ed pulse sequence for the resolution of the hydride spectral region with zero-quantum (ZQ) spectroscopy.[6] Spectral widths were 16000 and 2000 Hz in f$_2$ and f$_1$ dimensions, respectively. Datasets consisted of 16384 (f$_2$, complex) x 512 (f$_1$, real) points. Two scans were collected for each increment. Parahydrogen was bubbled through the sample for 1.5 s between scans. A 90°shifted square sine window function was applied in both dimensions and the f$_1$ dimension was zero filled to 4096 points before Fourier transformation. The dominant signal (#) in main text Fig. 1b and 2 represent complex **1** with three mtz ligands (i.e. [Ir(H$_2$)(IMes)(mtz)$_3$]Cl). This signal was omitted from 2D spectra during 2D processing by time-domain convolution filtering to avoid obscuring low concentrations signals.

## 5.	Evaluating residual NH₄⁺

In addition to evaluating ammonia in urine samples by 1D hyperpolarization experiments (Fig. 2, main text), residual ammonia was quantitatively evaluated by regular NMR. 60 µL of 100 mM DSS was added to 6 mL of pH adjusted urine (analogously to section 3a above), lyophilized and re-dissolved in 6 mL MilliQ water. pH was adjusted to pH 1 with 1 M HCl aq and a drop of D_2O was added. Ammonia was evaluated at 25 ℃ sample temperature under quantitative conditions with WATERGATE solvent suppression.
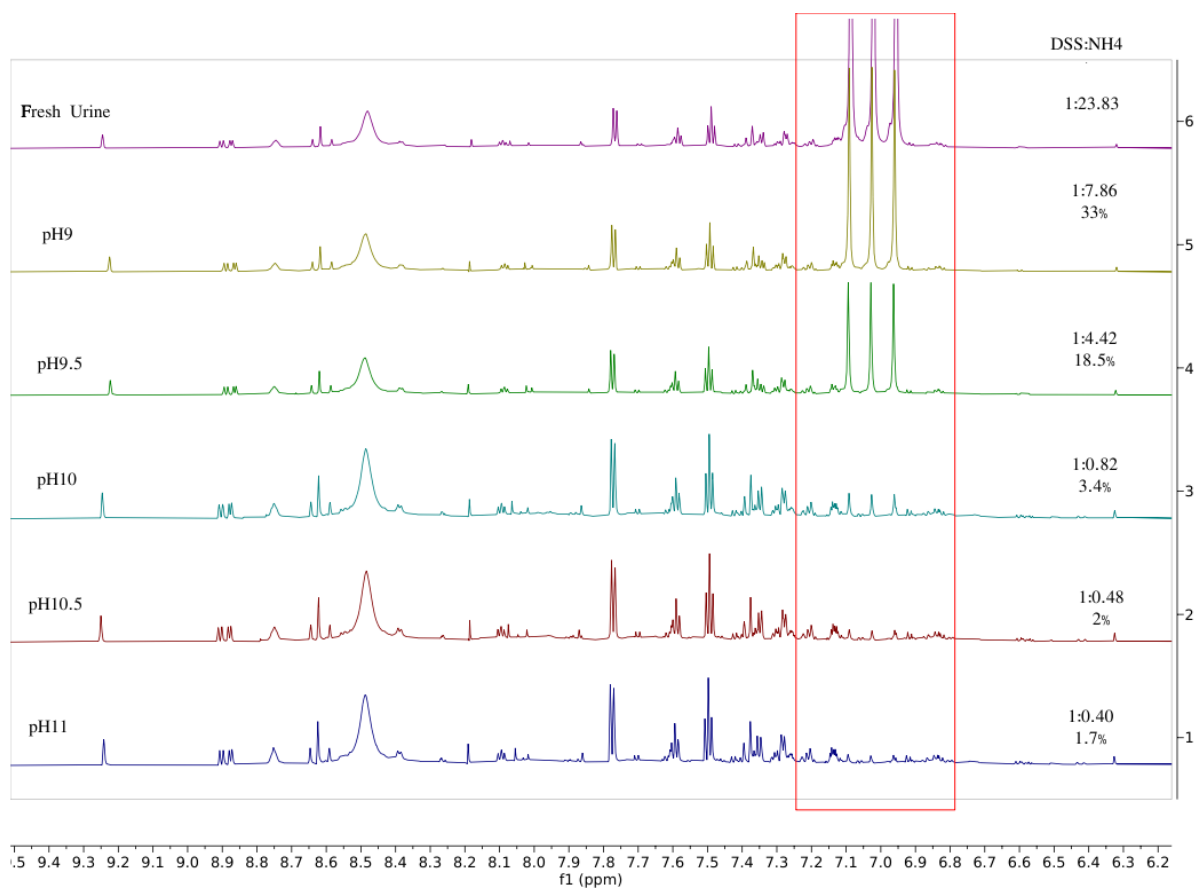
Fig. S1. Downfield region of urine (spectrum 6) and pH adjusted freeze-dried urine samples' (spectra 1-5) ¹H spectra at pH 1. The NH₄⁺ cation triplet at around 7 ppm (red box) has been integrated and compared to the integral DSS signal at 0 ppm to evaluate the amount of residual ammonia left (displayed in percent). Chemical shifts are referenced to DSS (not shown). Each spectra represents 16 scans.

6. Internal standard addition and quantification

Table S1. Integrals from 2D ZQ NMR plots (i.e. Figure 3 in main text) during an internal standard addition series[9] for 1-methyladenosine (m1a) and 3-hydroxycotoinine (3hc). Measured at 15 ^{0}C and at 6mM concentration of [Ir(Cl)(COD)(IMes)] with an 18-fold excess of mtz. The same information is represented graphically in Figure 4 in main text.

Standard addition point	m1a added (µM)	m1a integral (a.u.)	3hc added (µM)	3hc integral (a.u.)
1	0	9.65	0	114.35
2	1.57	19.71	1.99	156.70
3	3.14	38.37	3.99	251.23
4	4.71	50.76	5.98	302.12
5	5.81	58.25	-	-
Linear fit	y=8.72x+8.81		y=33.0x+107	

Standards were gravimetrically spiked into urine samples after sample preparation of section 3b. A new NMR sample was prepared for each data point. The relatively small tolerances between the individual data points and the linear fit demonstrate the robustness of the pH$_2$-HP process.

Concentration of the analyte (m1a or 3hc) in the NMR tube is calculated as follows:

$$y=ax + b$$

where a is the slope and b is the intercept. When y = 0 equation is solved for x, giving the analyte concentration prior to spiking.

The x value for m1a was 1.01 µM and for 3hc was 3.25 µM. In order to obtain analyte concentrations in urine the x value needs to be multiplied by 5, to consider dilution during NMR sample preparation.

7.   Identification of metabolites

As mentioned in article main text, assignment of hydride resonances that correspond to certain catalyst binding analytes can be challenging. Herein, a selection of analytes was identified by internal standard spiking and by comparing the chemical shifts and ZQ frequencies (i.e., in Fig. 3 in main text) from a urine sample spectrum with spectral data from pH_2-HP analysis of solutions of neat metabolites (as external standards). Chemical shifts of most metabolites' hydride signals proved to be tolerant of the changes in sample matrix when comparing neat solutions to urine samples.

The urine of Figure 3 (main text) was from a smoker – giving prior information. I.e., smoking related analytes were anticipated[3] (nicotine, cotinine, 3-hydroxycotinine). In addition, removing SPE from sample preparation allows to concurrently access potentially diagnostically valuable analytes that cannot be retained by the same SPE procedure – adenine, for instance.

Figures S2 – S10 below depict traces from hyperpolarized 2D spectra (i.e., Figure 3, main text) along the ZQ frequencies (f_1) of analyte hydride signals. Spectra for standard compounds were recorded at 5 µM analyte concentration in the NMR tube. Traces include all signals that share the same ZQ frequency. Achiral analytes produce a single pair of hydrides and are presented with a single pair of traces from a urine sample and from a standard sample. Chiral analytes (e.g., nicotine derivatives) can bind with the Ir-catalyst in two ways, giving rise to two diastereomeric complexes with individual hydride chemical shifts. Such complexes are compared by both of their hydride pairs. Hydride chemical shifts at the same f_1 frequency can be used as an identification tool. Some analytes (e.g., nicotine) display a slight matrix effect on the hydride chemical shifts. Identification can be double-checked with internal standard spiking, which has also been done for most analytes herein.
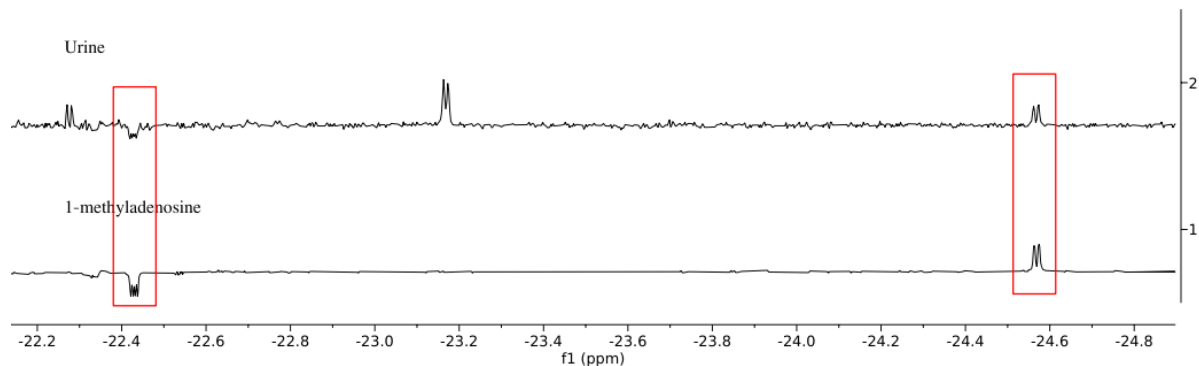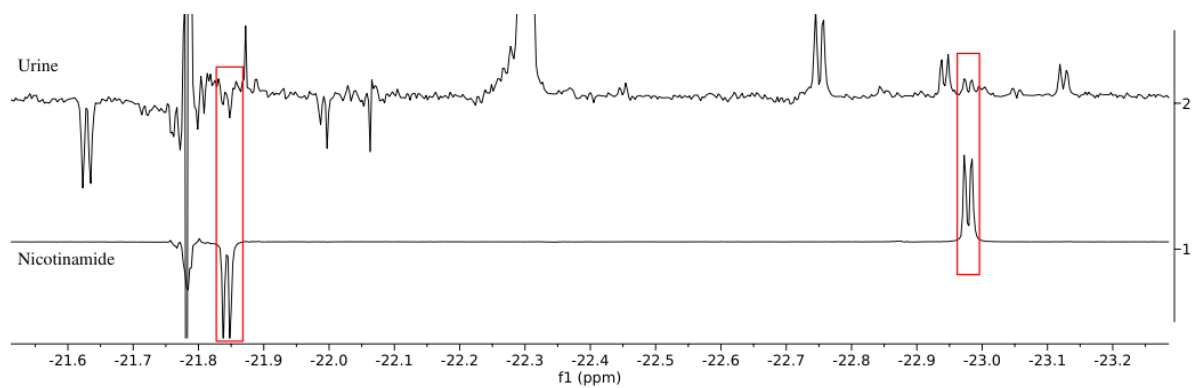

Fig. S2. Traces from 2D spectra at 1710 Hz f_1 frequency. Trace 1) represents 1-methyladenosine standard (one doublet pair); and trace 2) represents the same analyte in urine.
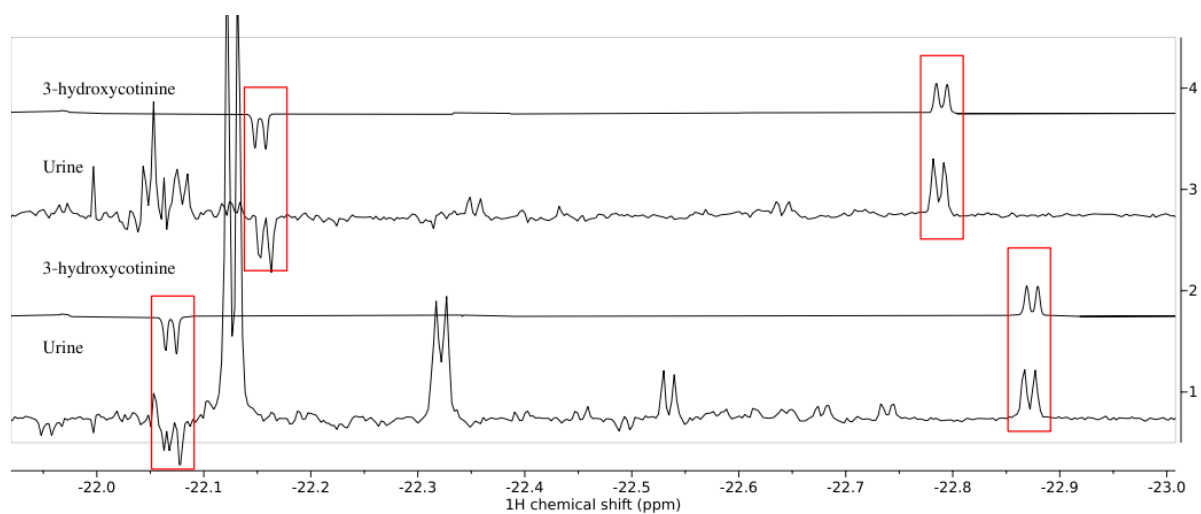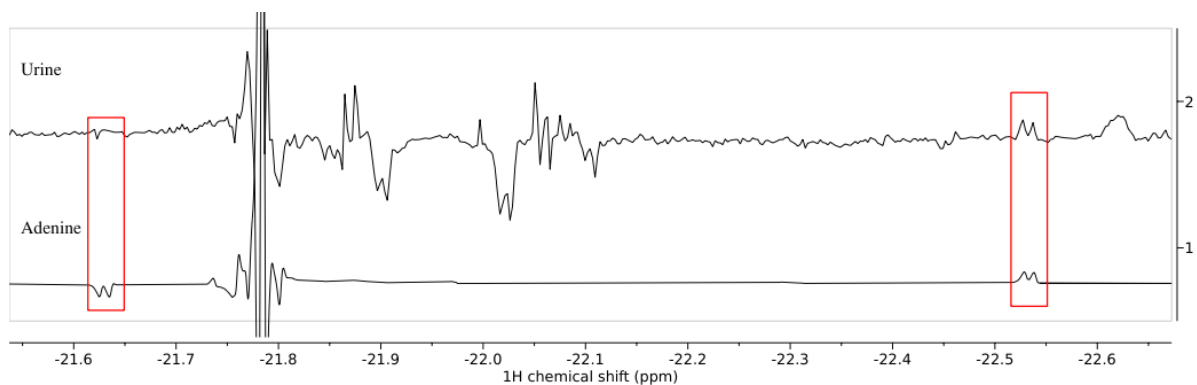
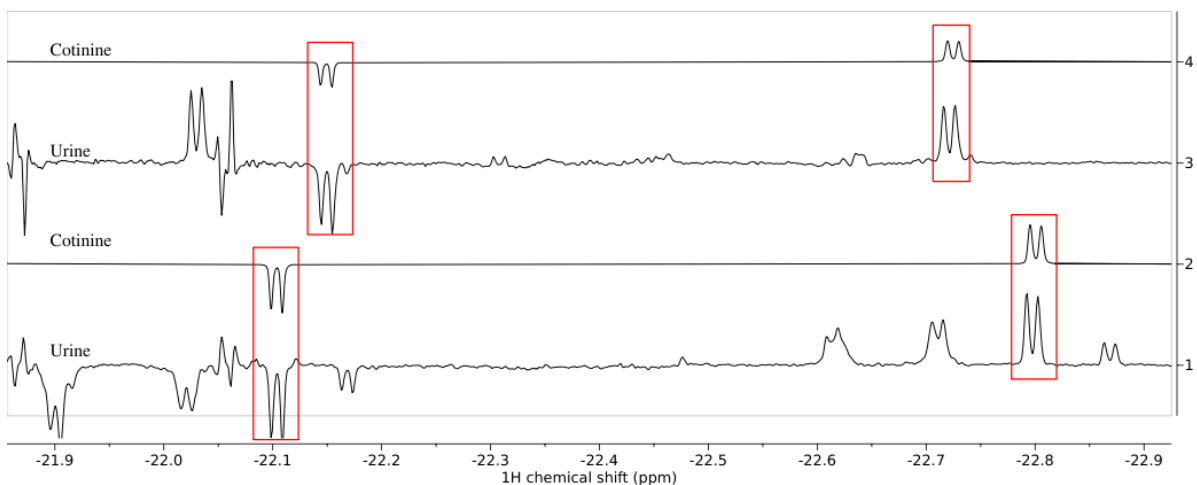**Fig. S3.** Traces from 2D spectra. Traces 2) and 4) represent 3-hydroxycotinine standard (two doublet pairs) at 639 Hz and 504 Hz f_1 frequency, respectively. Traces 1) and 3) represent the same analyte in urine.
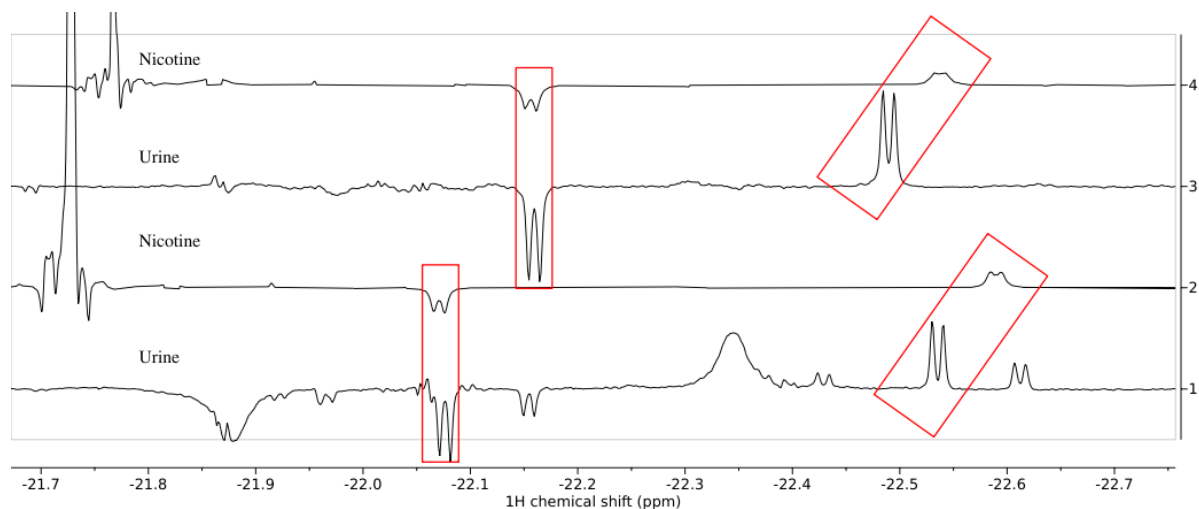

Fig. S4. Traces from 2D spectra at 910 Hz f_1 frequency. Trace 1) represents nicotinamide standard (one doublet pair); and trace 2) represents the same analyte in urine.

9

Fig S5. Traces from 2D spectra at 546 Hz f_1 frequency. Trace 1) represents adenine standard (one doublet pair); and trace 2) represents the same analyte in urine. Left hand signal in urine is obscured by noise ridges from dominating signals.
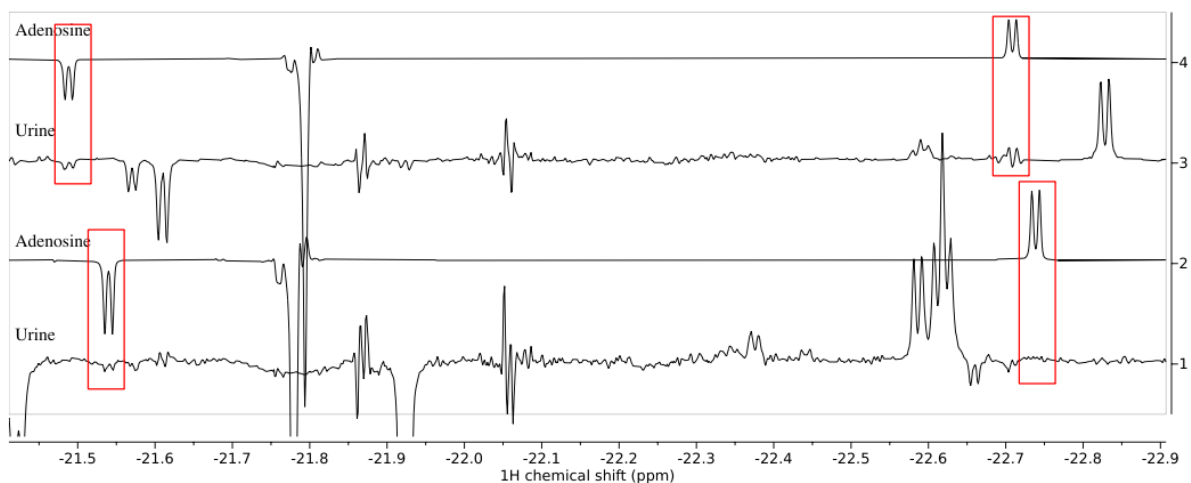

Fig S6. Traces from 2D spectra. Traces 2) and 4) represent cotinine standard (two doublet pairs) at 555 Hz and 458 Hz f_1 frequency, respectively. Traces 1) and 3) represent the same analyte in urine.
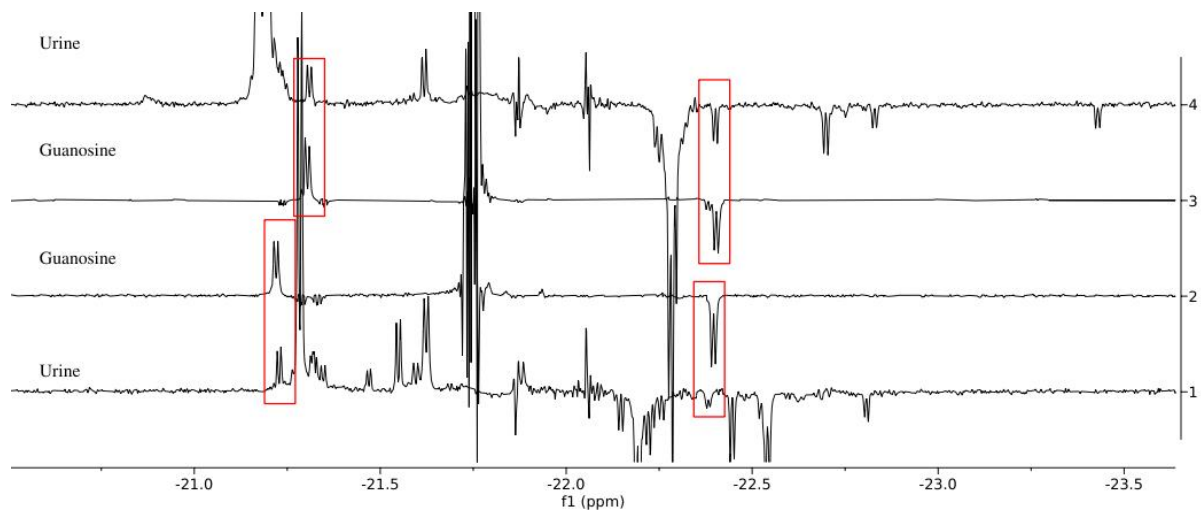
10

Fig. S7. Traces from 2D spectra. Traces 2) and 4) represent nicotine standard (two doublet pairs) at 368 Hz and 264 Hz f_1 frequency, respectively. Traces 1) and 3) represent the same analyte in urine. Note that the nicotine hydride lines are strongly shifted and much wider in standard solutions. The left-hand hydrides are *trans* to mtz in complex and are much less influenced. The right-hand signals are *trans* to analyte (nicotine, in this case). We suggest the differences between the behavior of nicotine and cotinine can be explained by their different basicity: the pyrrolidine ring of nicotine is a base and can be influenced by protonation in protic environments; the pyrrolidine ring has been turned into a lactam in cotinine, losing its basicity and making it much more immune to protonation.
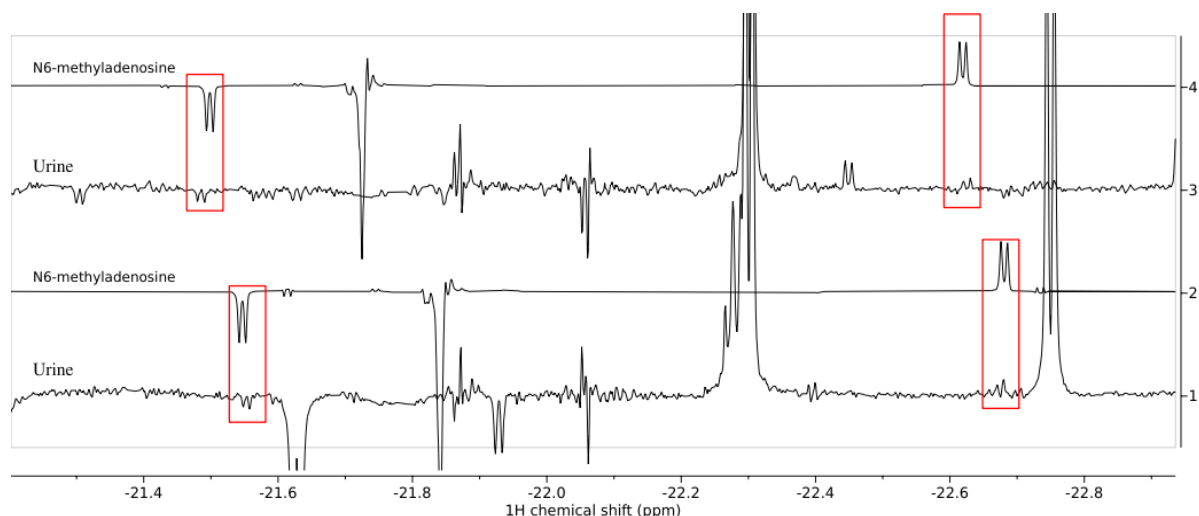
Fig. S8. Traces from 2D spectra. Traces 2) and 4) represent N6-methyladenosine standard (two doublet pairs) at 898 Hz and 913 Hz f_1 frequency, respectively. Traces 1) and 3) represent the same analyte in urine.

11

Fig. S9. Traces from 2D spectra. Traces 2) and 4) represent adenosine standard (two doublet pairs) at 977 Hz and 963 Hz f_1 frequency, respectively. Traces 1) and 3) represent the same analyte in urine. Right hand analyte signal in Trace 1 (urine) is obscured by the flank of a nearby larger signal.
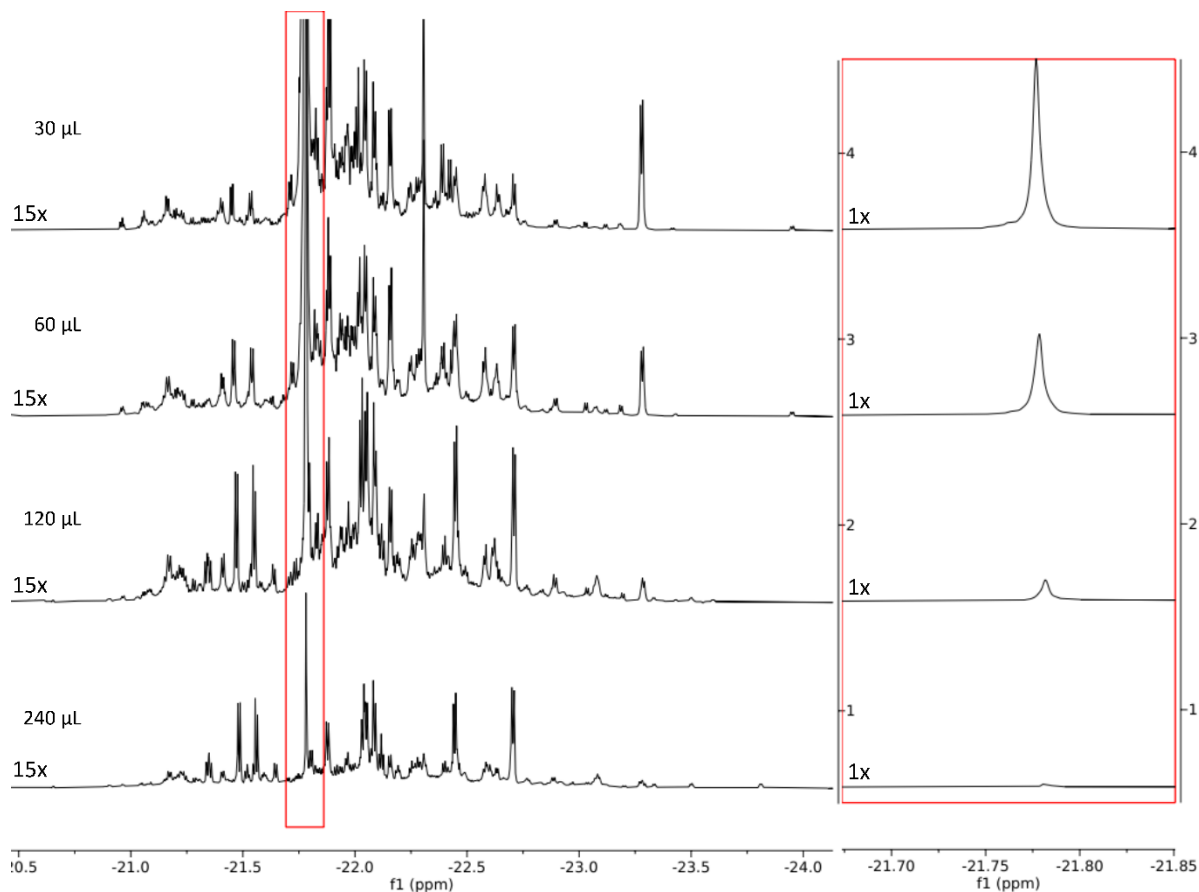

Fig. S10. Traces from 2D spectra. Traces 2) and 3) represent guanosine standard (two doublet pairs) at 873 Hz and 732 Hz f_1 frequency, respectively. Traces 1) and 4) represent the same analyte in urine.

8. Urine sample to catalyst ratio

Fig S11. An experiment to demonstrate the hydrides' signals when the catalyst system is forced out of its linear regime by introducing a too high combined analyte loading. Plot displays 1D SEPP[6–8] hydride spectra of different amounts of concentrated urine sample, prepared according to section 3b) above, in different ratios to a constant amount of iridium catalyst **1** (6mM) and **mtz** (18-fold excess over Ir-complex). Sample volume was always 600 µL.

Spectrum 4 above corresponds to 5-fold dilution of urine – the optimal conditions of this publication. Linear response to analyte concentration is maintained under 30 µL of urine sample as part of a 600 µL NMR sample (Fig. 4, main text). A 2-fold higher urine extract loading (60 µL, 2.5-fold dilution of urine in NMR sample) in spectrum 3 is borderline on the saturation point. Since we aimed to accommodate for concentration differences between different urine samples (i.e. from people with varying hydration levels) and also maintain capacity to increase certain analyte concentrations by spiking, 30 µL of urine sample for section 3b was deemed optimal.

13

A predictable and linear response of the catalyst system to changes in analyte concentration is maintained as long as the cumulative analytes' concentration is considerably below the co-substrate (mtz) concentration.[10] Under such conditions, the dominating form catalyst complex **1** is the symmetric complex [Ir(H$_2$)(IMes)(mtz)$_3$]Cl (at -21.78 ppm). That way the probability of forming a complex with more than one binding site occupied with an analyte (instead of mtz) is minimized. The right-hand inserts in Fig. S11 demonstrate the hydride peak of the complex with three mtz ligands. It's evident that when urine metabolome loading approximates original urine (spectrum 2) its signal is substantially decreased and almost disappears once the NMR sample becomes even more concentrated (spectrum 1).

9.   A brief comparison to SPE

Compared to prior SPE based works,[4,6,11] we had to increase catalyst loading fivefold while analyzing a fivefold diluted urine sample. This suggests we are analyzing a much more complex sample with a notably higher concentration of catalyst-interacting analytes. Moreover, prior SPE-based examples[4,6,11] used SPE to concentrate the compounds of interest from urine by five- to tenfold, instead of diluting fivefold. This supports the claim that the presented SPE-free approach is more universal and less selective. For illustrative purposes, we are referring to Figure S12 below that compares the results from the same hyperpolarized NMR experiment applied to an SPE extract and a sample prepared by the SPE-free approach. The latter presents more signal responses, corresponding to a larger number of different analyte-catalyst complexes formed. However, SPE allows to concentrate particular signals of interest, resulting more intense signals for particular targeted analytes (e.g., 1-methyl adenosine, m1a, in Figure S12).

Some of the compounds annotated in main text Fig. 3 would be very challenging to extract with a single SPE protocol. For instance, the lipophilic nicotine and hydrophilic adenine behave very differently in SPE processes. Concurrent hydrophobic SPE retention would require both analytes to be in neutral (isoelectric) state, which is achieved when sample pH is >2 units above both compounds strongest basic pKa and >2 units below both compounds strongest acidic pKa. Considering the strongest basic pKa of nicotine (8.58 according to hmdb.ca), its effective retention would require pH > 10.58. At the same time, retention of adenine would require pH < 8.23, since its strongest acidic pKa is 10.29 (according to hmdb.ca). Consequently, conditions for effective concurrent retention of both from aqueous biofluid to a common reverse phase SPE cartridge are unachievable. In contrast, both present very well in the sample preparation method of this work.
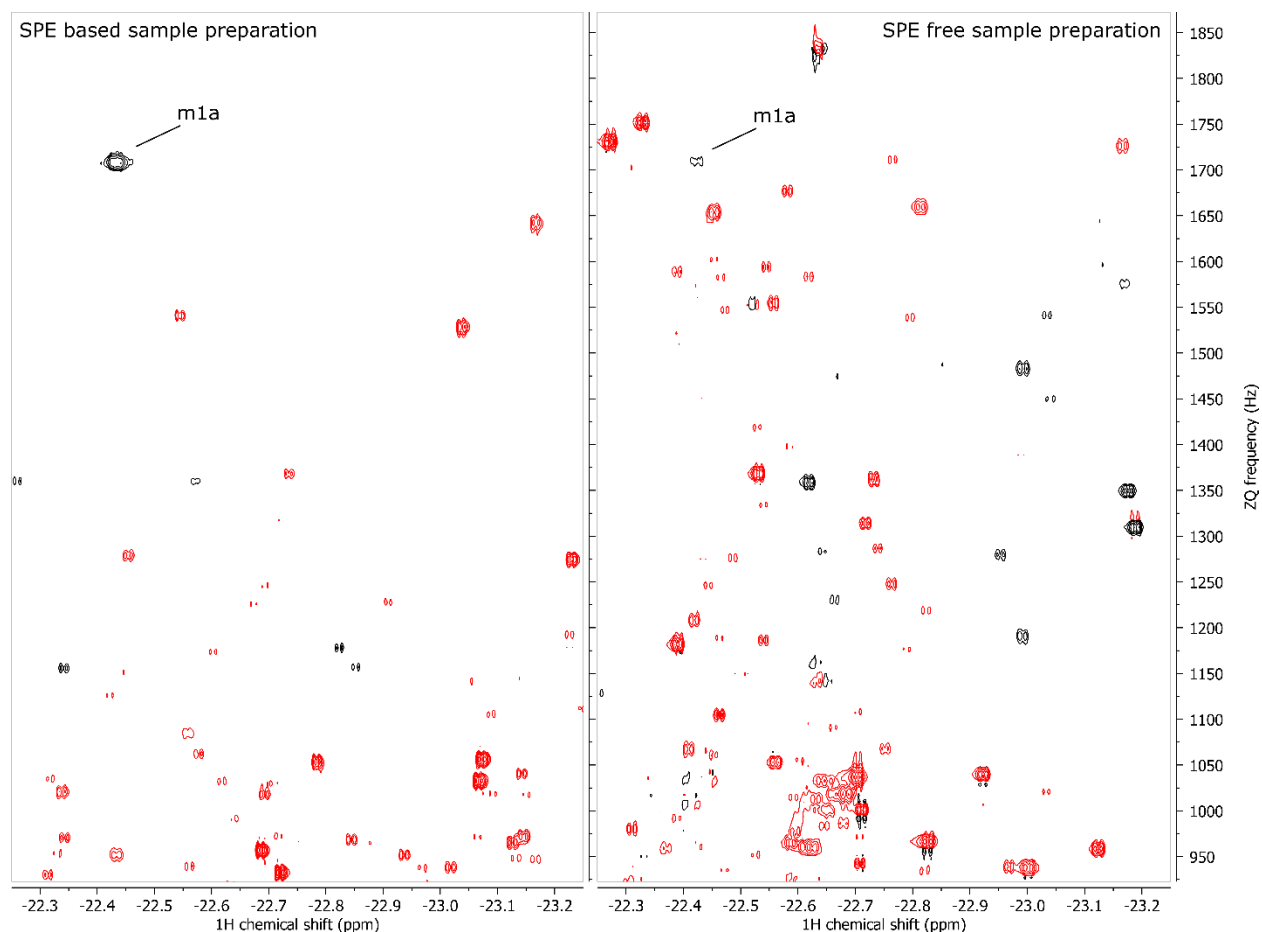
Figure S12. A comparison of a fragment from main text Fig. 3 and a similar spectrum from a methanolic SPE extract sample, prepared according to the method described for in our prior publication.[4]

10. Signal enhancement and sensitivity

The presented work utilizes the NMR detection scheme presented by Sellies et al.[6] Therein, the NMR methodology used here is reported to provide ca 1000-fold hydride signal enhancements for pyridine derivatives (e.g., nicotinamide) and down to 200-fold for more sterically bulky analytes with multiple binding modes (e.g., adenosine). The enhancements depend on the particular compound and sample conditions, but are expected to be in a similar order of magnitude in the work presented herein. Note that these values present the signal enhancements for the hydride signals which correlate to the concentration of catalyst bound analyte. Considering that not all molecules of a particular analyte are catalyst bound at any moment,[10] the hydride signals represent only a fraction of the analyte. Consequently, hydride signal enhancements are not equal to the hypothetical signal enhancement of the analyte compared to its native NMR signal

15

(between 0…10 ppm). This "overall" enhancement value would be challenging to measure in urine since we cannot resolve the dilute analyte signals more abundant metabolites by normal ^{1}H NMR to gauge their signal intensity.

To give a comparison of the sensitivities of different sample preparation approaches, we have recently estimated the Limit of Detection (defined and SNR=3) of an SPE-based urine analysis protocol to be 0.1 µM analyte concentration in an NMR tube.[4] Herein we measured an SNR of 55 for 3-hydroxycotinine in the NMR tube with the SPE-free sample preparation, which corresponded to (Fig. 4, main text) 3.25 µM analyte concentration. Comparison of these numbers suggests that the detection scheme sensitivities are comparable. However, since SPE allows to concentrate particular analytes, it allows to achieve detection of much lower concentration analytes.

11.   Chemoselectivity and analyte scope

Sample preparation presented here provides a much more analyte rich and wider scope sample than what is typically available by SPE. This, however, cannot be considered a totally global and universal protocol, since filtering by chemical properties of analytes exists on two levels: catalyst chemoselectivity and methanol solubility of analytes.

Methanol solubility questions arise upon reconstitution of the lyophilized sample. The observation that we have to centrifuge the sample after addition of methanol demonstrates that there are urine components that get expelled from the sample. We suggest this insoluble fraction includes some salts and protein, but certainly also some organic low-MW metabolites. The nature of these metabolites has not been determined yet.

Catalyst chemoselectivity wise, the used catalyst is the most widely used pH$_2$ chemosensing and SABRE hyperpolarization catalyst. Its known range of detectable analytes in constantly expanding as researchers explore its scope. Successful examples are known for several drugs,[4,11–13] nucleosides and nucleobases,[6,14] pyruvate,[15] tagged oligopeptides,[16,17] amino acids,[18,19] nitriles[20] and various heteroaromatic compounds,[21–23] including sulfur containing heteroaromatics[24] and the list keeps growing, demonstrating that the analyte scope of the current catalyst is rather wide. In parallel, efforts have been made to expand the analyte scope by designing completely new catalysts that would have entirely different analyte scope to detect new analyte classes. Notably, the Fout group published recently a cobalt-based catalyst for parahydrogen hyperpolarization of olefins.[25]

12. Reproducibility and sample stability

Adjusting urine sample pH to 11 can give rise to sample and analyte chemical stability concerns. We suggest that the realization of this risk is analyte dependent and would have to be considered in analytical method development. The risk, however, is not large: a study by Cook et al.[26] compared the stability of multiple drugs in urine samples at different pH levels. A variety of studied drugs were found to be stable over a three-day period at pH 10. At the same time, some specific drugs were gradually decomposing. Detectable loss of an analyte over 3 days at room temperature suggests that decomposition over minutes or hours is small. Likewise, we did not observe pH related sample stability issues during sample preparation at pH 11 for the analytes at that we have annotated in this proof-of-concept study.

The sample preparation protocol of SI chapter 3 above includes multiple steps that were not time-controlled very precisely: when multiple samples were prepared in parallel, the time durations of preparation steps for individual samples varied. This did not cause variability in the resulting spectra, suggesting that even if pH caused stability issues exist, the process is slow. For instance, the internal standard addition series for quantification (main text Fig. 4) was done with an individual sample for each datapoint, by standard addition to pH 11 treated samples prior to hyperpolarization experiment (e.g., after separate sample preparation). Considering that the standard addition itself is also an additional source of uncertainty, the notion that good linearity was maintained for the analytes that we followed suggests that sample stability was not an issue for these compounds.

13. References

1   R. Savka and H. Plenio, *Dalt. Trans.*, 2014, **44**, 891–893.

2   M. J. Cowley, R. W. Adams, K. D. Atkinson, M. C. R. Cockett, S. B. Duckett, G. G. R. Green, J. A. B. Lohman, R. Kerssebaum, D. Kilgour and R. E. Mewis, *J. Am. Chem. Soc.*, 2011, **133**, 6134–6137.

3   Seefeld, M. A.; Rouse, M. B.; Heerding, D. A.; Peace, S.; Yamashita, D. S.; McNulty, K. C. Inhibitors of AKT activity. WO Patent WO2008/098104 A1, 2008.

4   N. Reimets, K. Ausmees, S. Vija and I. Reile, *Anal. Chem.*, 2021, **93**, 9480–9485.

5   W. S. Law, P. Y. Huang, E. S. Ong, C. N. Ong, S. F. Y. Li, K. K. Pasikanti and E. C. Y. Chan, *Rapid Commun. Mass Spectrom.*, 2008, **22**, 2436–46.

6   L. Sellies, I. Reile, R. L. E. G. Aspers, M. C. Feiters, F. P. J. T. Rutjes and M. Tessari, *Chem. Commun.*, 2019, **55**, 7235–7238.

7   J. Barkemeyer, J. B. Argon, H. Sengstschmid, R. Freeman, J. Bargon, H. Sengstschmid and R. Freeman, *J. Magn. Reson. - Ser. A*, 1996, **120**, 129–132.

8   H. Sengstschmid, R. Freeman, J. Barkemeyer and J. Bargon, *J. Magn. Reson. Ser. A*, 1996, **120**, 249–257.

9   A. L. Hauswaldt, O. Rienitz, R. Jährling, N. Fischer, D. Schiel, G. Labarraque and B. Magnusson, *Accredit. Qual. Assur.*, 2012, **17**, 129–138.

10   N. Eshuis, N. Hermkens, B. J. a van Weerdenburg, M. C. Feiters, F. P. J. T. Rutjes, S. S. Wijmenga and M. Tessari, *J. Am. Chem. Soc.*, 2014, **136**, 2695–2698.

11   I. Reile, N. Eshuis, N. Hermkens, B. Weerdenburg, M. Feiters, F. Rutjes and M. Tessari, *Analyst*, , DOI:10.1039/C6AN00804F.

12   S. Glöggler, M. Emondts, J. Colell, R. Müller, B. Blümich and S. Appelt, *Analyst*, 2011, **136**, 1566–8.

13   H. Zeng, J. Xu, J. Gillen, M. T. McMahon, D. Artemov, J.-M. Tyburn, J. A. B. Lohman, R. E. Mewis, K. D. Atkinson, G. G. R. Green, S. B. Duckett and P. C. M. van Zijl, *J. Magn. Reson.*, 2013, **237**, 73–78.

14   J.-B. Hövener, N. Schwaderlapp, T. Lickert, S. B. Duckett, R. E. Mewis, L. a R. Highton, S. M. Kenny, G. G. R. Green, D. Leibfritz, J. G. Korvink, J. Hennig and D. von Elverfeldt, *Nat. Commun.*, 2013, **4**, 2946.

15   I. Adelabu, P. TomHon, M. S. H. Kabir, S. Nantogma, M. Abdulmojeed, I. Mandzhieva, J. Ettedgui, R. E. Swenson, M. C. Krishna, B. M. Goodson, T. Theis and E. Y. Chekmenev, *ChemPhysChem*, , DOI:10.1002/cphc.202100839.

16   T. Ratajczyk, T. Gutmann, P. Bernatowicz, G. Buntkowsky, J. Frydel and B. Fedorczyk, *Chem. - A Eur. J.*, 2015, **21**, 12616–12619.

17   T. Ratajczyk, G. Buntkowsky, T. Gutmann, B. Fedorczyk, A. Mames, M. Pietrzak, Z. Puzio and P. G. Szkudlarek, *ChemBioChem*, 2021, **22**, 855–860.

18   L. Sellies, R. L. E. G. Aspers and M. Tessari, *Magn. Reson.*, 2021, **2**, 331–340.

19   A. N. Pravdivtsev, G. Buntkowsky, S. B. Duckett, I. V. Koptyug and J.-B. Hövener, *Angew. Chemie Int. Ed.*, 2021, anie.202100109.

20   R. E. Mewis, R. A. Green, M. C. R. Cockett, M. J. Cowley, S. B. Duckett, G. G. R. Green, R. O. John, P. J. Rayner and D. C. Williamson, *J. Phys. Chem. B*, 2015, **119**, 1416–1424.

21   N. Eshuis, R. L. E. G. Aspers, B. J. A. van Weerdenburg, M. C. Feiters, F. P. J. T. Rutjes, S. S. Wijmenga and M. Tessari, *Angew. Chemie Int. Ed.*, 2015, **54**, 14527–14530.

22   N. Eshuis, B. J. A. van Weerdenburg, M. C. Feiters, F. P. J. T. Rutjes, S. S. Wijmenga and M. Tessari, *Angew. Chemie Int. Ed.*, 2015, **54**, 1481–1484.

23   V. Daniele, F.-X. Legrand, P. Berthault, J.-N. Dumez and G. Huber, *ChemPhysChem*, 2015, **16**, 3413–3417.

24   R. V. Shchepin, D. A. Barskiy, A. M. Coffey, B. M. Goodson and E. Y. Chekmenev, *ChemistrySelect*, 2016, **1**, 2552–2555.

25   S. R. Muhammad, R. B. Greer, S. B. Ramirez, B. M. Goodson and A. R. Fout, *ACS Catal.*, 2021, **11**, 2011–2020.

26   J. D. Cook, K. A. Strauss, Y. H. Caplan, C. P. LoDico and D. M. Bush, *J. Anal. Toxicol.*, 2007, **31**, 486–496.